

# Thermal characterization of some guanylhydrazones by thermal and nonthermal techniques

F. P. Galvão · W. A. De Brito · M. G. Dantas · M. A. V. Pereira ·  
J. X. Araújo-Júnior · P. H. B. França · A. E. G. Santana · R. O. Macêdo ·  
E. A. N. Ribeiro · E. G. Barbosa · C. F. S. Aragão · A. P. B. Gomes

Received: 17 July 2014 / Accepted: 28 November 2014 / Published online: 24 December 2014  
© Akadémiai Kiadó, Budapest, Hungary 2014

**Abstract** 2-[(3,5-di-*tert*-butyl-4-hydroxyphenyl)methylene]-hydrazinecarboximidamide (WE010), 2-[(1,1'-biphenyl)-4-ylmethylene]-hydrazinecarboximidamide (WE014), and 2-[(3,4-dichlorophenyl)methylene]-hydrazinecarboximidamide (WE017) are guanylhydrazone derivatives widely studied biologically and chemically; however, there are no studies regarding their thermal behaviors. The present study aims to apply the thermal analyses: differential scanning calorimetry (DSC), differential scanning calorimetry coupled to the photovisual system (DSC-photovisual), and thermogravimetry (TG), to characterize the guanylhydrazones, as well as HPLC and FTIR. The DSC curve of WE010 shows a melting process with  $T_{\text{onset}}$  at 190 °C and peak at 193.5 °C ( $\Delta H$  41.0 J g<sup>-1</sup>). Due to the symmetry of the melting peaks obtained by DSC, it is possible to calculate the purity of the sample (98.87 %). The DSC curve of WE014 shows the melting process in the range of 208–213 °C, with a melting peak at 211 °C ( $\Delta H$  61 J g<sup>-1</sup>).

The DSC curve of WE017 showed  $T_{\text{onset}}$  at 215 °C and peak temperature of 219 °C ( $\Delta H$  55 J g<sup>-1</sup>). The TG curve of WE010, WE014, and WE017 presents initial decomposition temperatures of 186.95, 197.31, and 195.44 °C, respectively. The DSC-photovisual confirmed the results of DSC and TG. The HPLC determined the purities of the samples and confirmed the results of DSC. The FTIR confirmed the thermal data. Thus, the use of thermal analysis is an important tool for the characterization of molecules with therapeutic potential contributing to the characterization and evaluation of their stability as well as nonthermal technique with complementary tool.

**Keywords** Guanylhydrazones · DSC · TG · HPLC · FTIR

## Introduction

The knowledge of the physicochemical properties of drugs is an essential variable during the development of pharmaceutical products. The rational design of the pharmaceutical form should, however, start with the characterization of the active pharmaceutical ingredients (APIs) in question, in order to improve the quality parameters of the pharmaceutical products. The process involving the research and development of new drugs has increased markedly, and there is a great need for the development of new pharmacologically active compounds that are effective against different pathologies even without treatment, which can replace those existing and reduce costs as well as any side effects [1].

The method for drug discovery based on structural modification of known molecules leads to the characterization of new compound prototypes that act by the same mechanism as that of the drug molecule origin. This

---

F. P. Galvão · W. A. De Brito · M. G. Dantas ·  
M. A. V. Pereira · E. G. Barbosa · C. F. S. Aragão ·  
A. P. B. Gomes (✉)  
Laboratory Quality Control (LCQMed), Pharmaceutical  
Sciences Department, Federal University of Rio Grande do  
Norte – UFRN, Av. General Cordeiro de Faria s/n, Petrópolis,  
Natal, Rio Grande do Norte 59000-000, Brazil  
e-mail: ana.pbgomes@gmail.com

J. X. Araújo-Júnior · P. H. B. França ·  
A. E. G. Santana · E. A. N. Ribeiro  
ESEN FAR, Federal University of Alagoas, Av. Lourival de  
Mello Motta, s/n, Tabuleiro dos Martins, Maceió,  
AL 57072-970, Brazil

R. O. Macêdo  
Unified Laboratories of Development and Assays of  
Medicines – LUDEM, Federal University of Paraíba – UFPB,  
Camps 1, João Pessoa, PB 58059-900, Brazil

approach is widely employed in the pharmaceutical industry to research new drugs. However, only the discoveries of new bioactive substances, which may represent authentic innovative chemical entities, make possible therapeutic application, which characterizes pharmaceutical innovation [2].

Taking this approach, compounds derived of guanlylhydrazones have shown promising biological effects that are of pharmacological interest. The guanlylhydrazones represent a group of compounds comprising different chemical classes containing amidine groups (guanlyl) connected to the hydrazone group [3]. Guanlylhydrazones are molecules widely studied, biologically and chemically. In chemistry, they are used as intermediates in the construction of heterocyclic compounds, polyfunctional and containing atoms of nitrogen [4]. Since the last decade, hundreds of guanlylhydrazones derivatives were synthesized and their structure–activity relationship has been extensively studied—especially in relation to its action—trypanosomiasis african [5–8]. In addition, they also have an interesting action against pneumocystosis, and the antitumor effects of these substances are remarkable [3, 8]. There are several reports of guanlylhydrazones being studied as antihypertensives [9, 10], antidiabetic [11, 12], antitumor [8, 9], antibacterial [3, 13, 14], antimalarials [15], and trypanocidal [6, 16, 17].

Andreani et al. [8] reported the synthesis of new guanlylhydrazones that have been tested as potential antitumor agents in the cells of lung cancer, breast cancer, and glioma. Moreover, Andreani et al. concluded that 3-nitrophenyl and 4-nitrophenyl are important pharmacophoric groups for this activity. However, there are no thermal studies with these new guanlylhydrazones.

The guanlylhydrazones studied in this research had their therapeutic potential in human tumor cell lines evaluated, with much activity with respect to inhibiting the growth of neoplastic cells following strains tested: human colon (HCT-8), melanoma (MDA-MB435), glioblastoma (SF -295), and promyelocytic leukemia (HL-60), with the results of high cytotoxicity in tumor cells in vitro inhibition being shown to be very satisfactory, between 97 and 100 % [18]. The structures of guanlylhydrazones studied in this study are the following:

Thermogravimetry (TG) and differential scanning calorimetry (DSC) are thermal techniques widely distributed and used in pharmaceutical analyses. These techniques are used in studies of drug characterization, purity, compatibility studies, polymorphism identification, stability evaluation, thermal decomposition of drugs, and development of pharmaceutical formulations [19–26].

Thermal analysis of pharmaceutical/medicinal compounds is a reliable method for purity control, and it is a necessary part of the characterization of new compounds

with potential bioactivity. The thermal analysis methods are widely used for the study of the stability and the decomposition of the substances used in medicine. The evaluation of the stability of biologically active compounds in solid dosage form is carried out specifically by analyzing its decompositional behavior in isothermal and nonisothermal conditions [27]. Some studies that evaluate thermal behaviors of the newly synthesized biologically active compounds are reported [28–32].

Some authors had studied other guanlylhydrazones by HPLC [33, 34]. Other analytic non-thermal techniques have been used to identify and quantify samples with HPLC and FTIR [35, 36]. However, there are no studies with these guanlylhydrazones by techniques cited above.

This study aims to characterize the molecules of guanlylhydrazones 2-[(3,5-di-*tert*-butyl-4-hydroxyphenyl)methylene]-hydrazinecarboximidamide (WE010), 2-([1,1'-biphenyl]-4-ylmethylene)-hydrazinecarboximidamide (WE014), and 2-[(3,4-dichlorophenyl)methylene]-hydrazinecarboximidamide (WE017) by applying the thermal techniques TG, DSC, and differential scanning calorimetry coupled to photovisual system (DSC-photovisual), HPLC, and FTIR (Fig. 1).

## Materials and methods

### Materials

The guanlylhydrazones WE010, WE014, and WE017 were utilized in this study (Fig. 1). They belong to the class of aromatic guanlylhydrazones. It was synthesized by a direct reaction of the respective aldehyde with aminoguanidine hydrochloride in refluxing 95 % ethanol using an adaptation of the methodology according to Ulrich and Cerami [5], which describes the condensation of an equimolar carbonylated derivative, aldehyde or ketone type, with

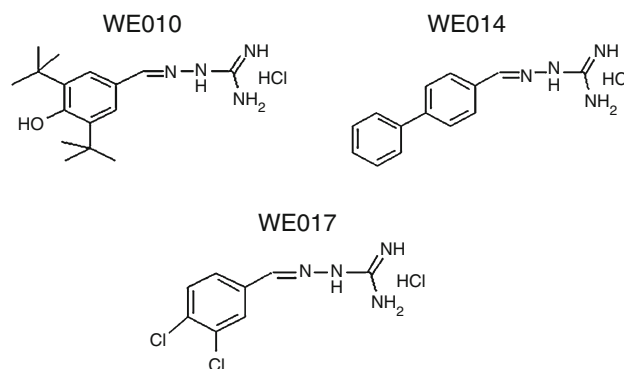


**Fig. 1** Chemical structures of guanlylhydrazones WE010, WE014, and WE017

aminoguanidines in an alcoholic medium under reflux, and catalytic amounts of acid [18].

#### Thermogravimetry (TG)

The dynamic thermogravimetric curves of the samples were recorded using a thermobalance (Shimadzu, model TGA-50) with an alumina crucible. The apparatus was calibrated with calcium oxalate monohydrate. Rising temperature experiments were conducted in the temperature range of 25–900 °C at heating rates of 10, 20, 40, 60, and 80 °C min<sup>-1</sup> at nitrogen flow rate of 50 mL min<sup>-1</sup> with the sample mass being in the 5.0 ± 0.5 mg range. The TG curves were analyzed using the TASYs software from Shimadzu.

#### Differential scanning calorimetry (DSC)

DSC curves of samples were recorded with a differential scanning calorimeter (Shimadzu, model DSC-50) using a closed aluminum crucible. The apparatus was calibrated using indium (156.6 ± 0.3 °C) as the standard. The heat flow signal was calibrated by the melting heat rate of indium (28.59 ± 0.3 J g<sup>-1</sup>). A rising temperature experiment was conducted in the temperature range of 25–400 °C at heating a rate of 10 °C min<sup>-1</sup> at nitrogen flow rate of 50 mL min<sup>-1</sup> with the sample mass being in the 2.0 ± 0.1 mg range. The DSC curves were analyzed using the TASYs software from Shimadzu for determination of temperature of melting, enthalpy and purity. The purity was determined using the Van't Hoff equation.

#### Differential scanning calorimetry (DSC) coupled to a photovisual system

DSC-photovisual data were recorded with a differential scanning calorimeter (Shimadzu, model DSC-50) coupled to the photovisual system, equipped with a microscope (Olympus, model SZ-CTV60) and a camera (Sony, model VCC-520). The samples were placed into an open aluminum crucible and heated in the temperature range 25–400 °C at a heating rate of 10 °C min<sup>-1</sup> under the same conditions of the nitrogen flow from a conventional DSC. The pictures were taken by the Asymetrix DVP 4.0 program in real time to observe the phase transitions in the samples.

#### High-performance liquid chromatography (HPLC)

The LC method was performed on a HPLC SYKAM system equipped with a S7131 pump and a S3240 photodiode array (PDA) detector. The peak areas were integrated automatically by computer using a Clarity software

program. The experiments were performed on a reversed phase ACE C18 column (150 mm × 4.6 mm). The chromatographic system was operated isocratically at ambient temperature, using a mobile phase of acetonitrile:water (30:70, v/v), run at a flow rate of 1.6 mL min<sup>-1</sup>, and using PDA detector at 290 nm. The injection volume was 20 µL. Compounds were identified by their absorption spectra. In the preparation of guanylhidrazone solution, each guanylhidrazone solution was prepared with mobile phase, in a concentration of 500 µg mL<sup>-1</sup>.

#### Fourier-transformed-infrared spectroscopy (FTIR)

The spectra of the individual compounds were performed on an ATR-FTIR spectrometer (IRprestige-21 Shimadzu) between 700 and 4,000 cm<sup>-1</sup>, at an optical resolution of 1.0 cm<sup>-1</sup> and averaged over 20 scans.

The MID spectra obtained for the samples subjected to different temperatures were compared using an ad hoc algorithm [37]. This algorithm calculates correlations of successively increasing data points' numbers from the two spectra and plots the results as peaks that indicate region with low similarity. The correlation as low as 0.5 was considered as an indication that the samples suffered degradation upon heating.

## Results and discussion

### Thermal analysis

Figure 2 displays TG curves of WE010, WE014, and WE017 at the heating rates of 10, 20, 30, 40, and 50 °C min<sup>-1</sup>. At the heating rate of 10 °C min<sup>-1</sup>, the TG curve of WE010 (Fig. 2a) showed four mass loss stages with the first stage corresponding to the decomposition of WE010, the mass loss of which was of 25 %. The WE010 was thermally stable up 187 °C. The other three stages presented the following mass losses: 42, 21, and 12 %, respectively (Table 1). At the heating rate of 20 °C min<sup>-1</sup>, the WE010 also showed four steps temperature of decomposition of which was 197 °C. Then, happened the increasing of temperature as the heating rate increases. This behavior was observed for all heating rates and all stages, as noted in Table 1. Figure 2b displays that the TG curve of WE014, at the heating rate of 10 °C min<sup>-1</sup>, consists of six stages, and the first stage can be attributed to the loss of solvent residue or moisture, which corresponds to about 6 %. The second stage corresponded to the decomposition of WE014 and displayed initial temperature of 197 °C, at the heating rate of 10 °C min<sup>-1</sup>, with the mass loss of 23 %. Other four stages showed losses of 29, 15, 18, and 6 %, respectively (Table 2). Figure 2c

**Fig. 2** TG curves of guanylhydrazones of **a** WE010, **b** WE014, and **c** WE017

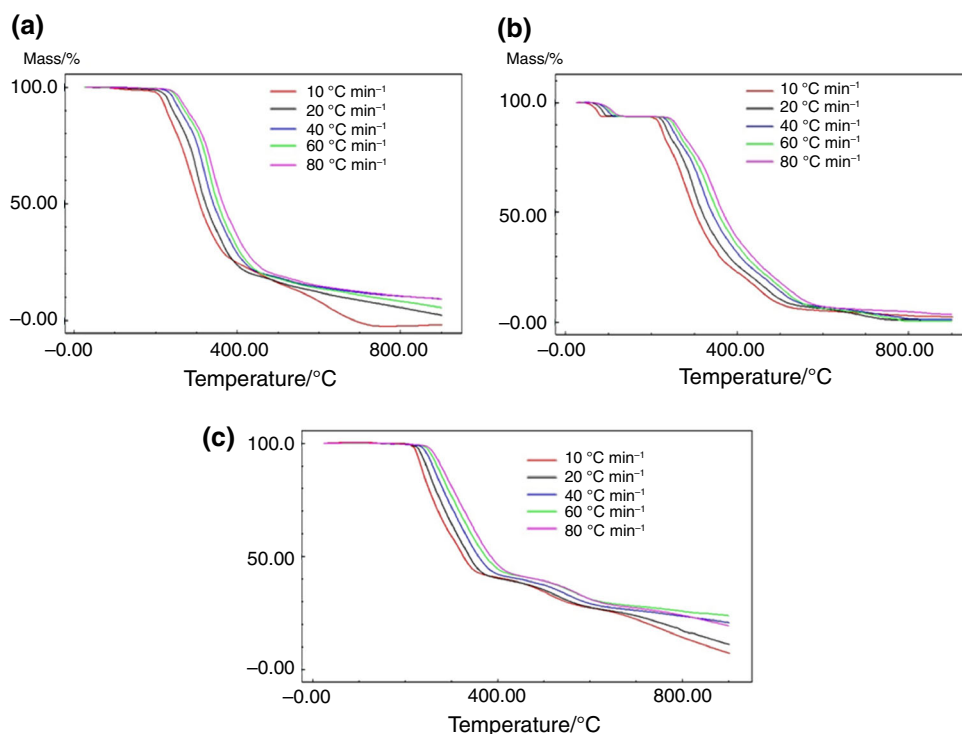


**Table 1** TG curves of WE010 at the heating rates of 10, 20, 40, 60, and 80 °C min<sup>-1</sup> under flow of nitrogen at 50 mL min<sup>-1</sup>

Heating rates/°C min <sup>-1</sup>	1st step			2nd step			3rd step			4th step		
	$T_i$ /°C	$T_e$ /°C	Mass loss/%	$T_i$ /°C	$T_e$ /°C	Mass loss/%	$T_i$ /°C	$T_e$ /°C	Mass loss/%	$T_i$ /°C	$T_e$ /°C	Mass loss/%
10	187	265	25	265	357	42	357	581	21	581	892	12
20	197	283	23	283	321	25	321	395	26	395	892	22
40	213	300	23	300	335	23	335	418	29	418	892	15
60	224	308	21	308	361	32	361	425	21	425	892	19
80	225	316	21	316	361	27	361	435	25	435	892	17

$T_i$  initial temperature,  $T_e$  end temperature

demonstrates that the TG curve of WE017 was thermally stable up 195 °C, at the heating rate of 10 °C min<sup>-1</sup>. There were six mass loss stages for the heating rates of 10 and 20 °C min<sup>-1</sup>. There were five mass loss stages for 30, 40, and 50 °C min<sup>-1</sup>. With the enhancing heating rate, fusion during the fifth and sixth stages happened for WE017. Other data are indicated in Table 3. The initial temperature increases with the enhancing heating rates for all the compounds.

Figure 3 presents the DSC curves of WE010, WE014, and WE017. The DSC curve of WE010 demonstrated endothermic four-phase transitions: the first transition starts at 91.5 °C; the peak maximum occurs at 95 °C, with an enthalpy value of about 2.5 J g<sup>-1</sup>. The melting peak is very characteristic, presenting itself as an endothermic peak with  $T_{\text{onset}}$  at 190 °C and  $T_{\text{peak}}$  at 193.5 °C with an enthalpy

value of 41.0 J g<sup>-1</sup>. DSC curve of WE014 showed an endothermic process characteristic of melting in the range of 208–213 °C, with a melting peak at 211 °C and enthalpy value of 61 J g<sup>-1</sup>. In addition, the DSC curve of WE017 showed four-phase transitions, where findings indicated an endothermic process characteristic of melting at the onset of 215 °C and peak temperature of 219 °C, as well as an enthalpy value of 55 J g<sup>-1</sup>. There was no possibility of determining the purities of the samples WE014 and WE017 because the melting occurred following decomposition, without complete recovery of the baseline. However, we believe that the WE010 sample is more impure, and those two endothermic peaks after melting are attributed to the impurities, that in this case, are WE014 and WE017, which peak at exactly the related temperatures of the samples (Fig. 2). The sample WE014 presented as an impurity in

**Table 2** TG curves of WE014 at the heating rates of 10, 20, 40, 60, and 80 °C min<sup>-1</sup> under nitrogen flow

Heating rates/ °C min <sup>-1</sup>	1st step		2nd step		3rd step		4th step		5th step		6th step	
	T <sub>i</sub> /°C	T <sub>e</sub> /°C	T <sub>i</sub> /°C	T <sub>e</sub> /°C	T <sub>i</sub> /°C	T <sub>e</sub> /°C	T <sub>i</sub> /°C	T <sub>e</sub> /°C	T <sub>i</sub> /°C	T <sub>e</sub> /°C	T <sub>i</sub> /°C	T <sub>e</sub> /°C
10	39	86	197	265	265	322	29	322	377	500	500	896
20	39	107	213	275	275	323	26	323	381	509	509	896
40	39	117	218	297	297	354	27	354	406	538	538	896
60	39	132	233	305	305	365	28	365	429	552	552	896
80	39	141	234	322	322	383	28	383	451	564	564	896

T<sub>i</sub> initial temperature, T<sub>e</sub> end temperature

**Table 3** TG curves of WE017 at the heating rates of 10, 20, 40, 60, and 80 °C min<sup>-1</sup> under nitrogen flow

Heating rates/ °C min <sup>-1</sup>	1st step		2nd step		3rd step		4th step		5th step		6th step	
	T <sub>i</sub> /°C	T <sub>e</sub> /°C	T <sub>i</sub> /°C	T <sub>e</sub> /°C	T <sub>i</sub> /°C	T <sub>e</sub> /°C	T <sub>i</sub> /°C	T <sub>e</sub> /°C	T <sub>i</sub> /°C	T <sub>e</sub> /°C	T <sub>i</sub> /°C	T <sub>e</sub> /°C
10	195	257	257	346	346	456	7	456	561	677	677	892
20	209	283	283	361	361	481	7	481	573	708	708	892
40	209	287	287	380	380	492	7	492	595	892	892	892
60	218	299	299	395	395	516	7	516	612	892	892	892
80	224	307	307	400	400	520	8	520	620	892	892	892

T<sub>i</sub> initial temperature, T<sub>e</sub> end temperature



**Fig. 3** DSC curves of WE010, WE014, and WE017

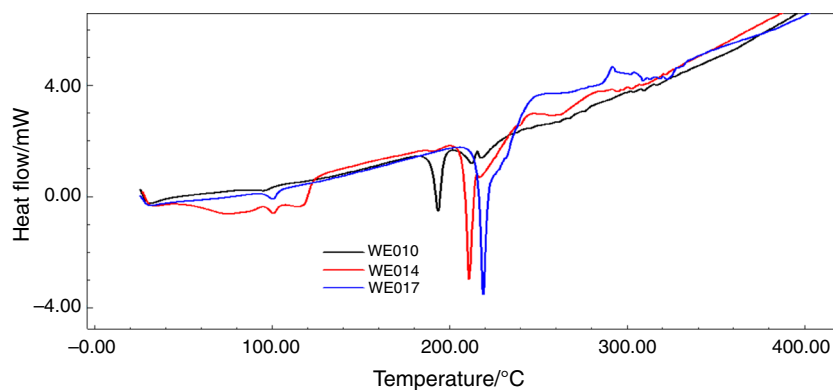
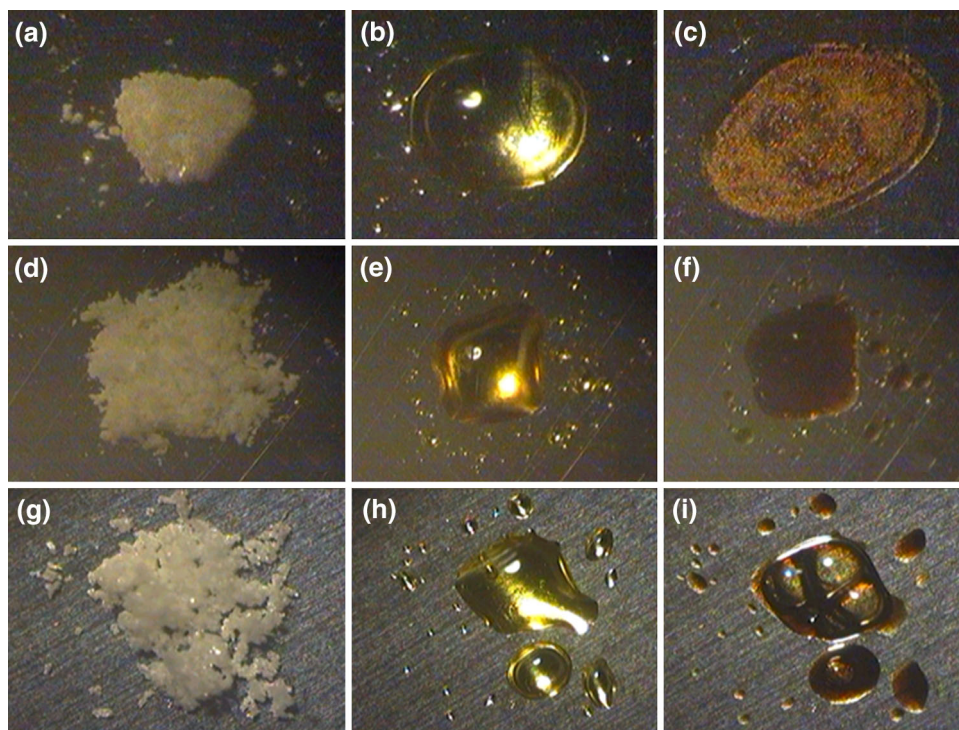


**Fig. 4** DSC-photovisual of WE010 (a environment, b 196 °C, and c 340 °C); WE014 (d environment, e 201 °C, and f 350 °C); and WE017 (g environment, h 222 °C, and i 400 °C)



the WE010 and WE017, and WE017 does not have the other two samples as impurities (Fig. 2).

Araújo et al. have used DSC for determining the purity of substances with a fast and reliable technique for eutectic systems, in which melting is not accompanied by thermal decomposition of the material. Those authors found that the main advantages of the DSC, over chromatography and spectroscopy, are that the analysis of all the impurities normally does not require standards except, for the main compound, and permits simultaneous measurements of the melting range and variation of enthalpy [35]. The sample WE010 showed a purity of 98.87 %.

Many authors have used the thermal and nonthermal techniques in the physicochemical characterization of herbal products [35], as well as of other synthetic

substances with biological activity potential [28–32]. All those studies showed the relevance of the thermal analysis in the determinations of the thermal parameters and stabilities of those products.

Differential scanning calorimetry (DSC) coupled to a photovisual system

Figure 4 displays the WE010 at room temperature (Fig. 4a) without any visible changes. Melting can be visualized at 196 °C (Fig. 4b), with the appearance of a precipitate. Its decomposition is complete at 340 °C (Fig. 4c). Figure 4 also shows the WE014 without any visible changes at room temperature (Fig. 4d) and melting at 201 °C (Fig. 4e). The completion of decomposition of WE014 occurred at

350 °C (Fig. 4f). The WE017 can be observed at room temperature (Fig. 4g), and its melting at 222 °C (Fig. 4h). The decomposition of the WE017 (Fig. 4i) occurred at 400 °C. Other authors also used DSC coupled to a photo-visual system [22–25] and confirmed the parameters obtained by DSC and TG. This technique is an important tool to confirm events in special melting.

#### High-performance liquid chromatography (HPLC)

HPLC is an established technique for the separation and quantification of the samples. Other characteristic parameter attributed a chromatography is purity determination, but actually no DSC technique has been also used for this finality [36].

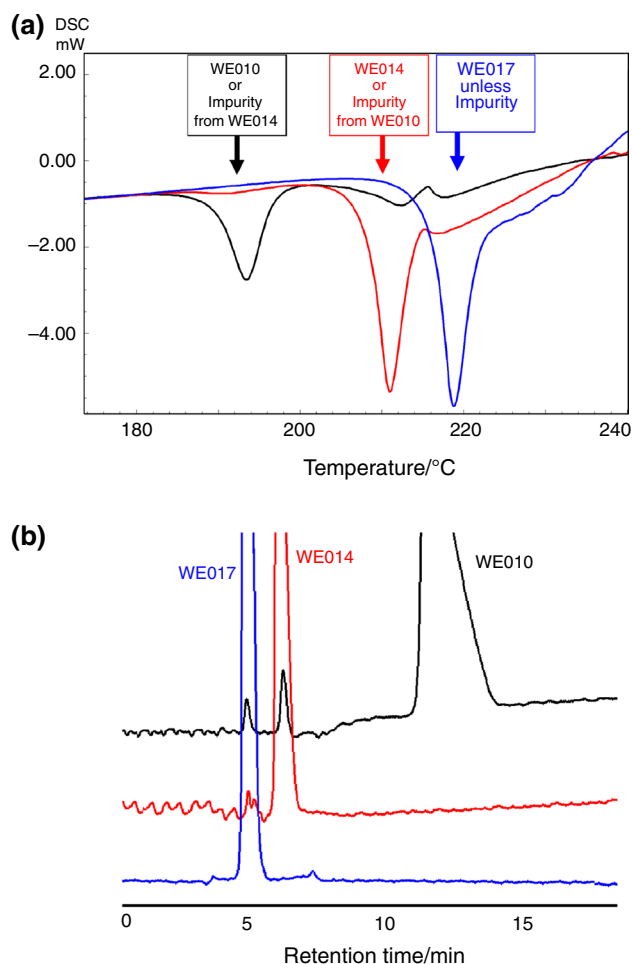
Previously, Araújo et al. determined the purity by DSC for samples melting of which is complete. However, we could characterize our samples using DSC, and HPLC confirmed the resulting information, as can be seen in Fig. 5.

Figure 5a also shows that the WE010 sample presented the melting peak followed by two endothermic peaks, which are attributable to WE014 and WE017, since the overlap of peaks found in the temperature WE010 exactly the same. The sample presents WE014 and WE017 as impurities. WE017 is not present in the other two samples, but its decomposition is through sequential melting, which does not allow for the determination of its purity. This information is confirmed by HPLC. Figure 5b shows the chromatographic peak corresponding to the WE010 sample and its impurities (WE014 and WE017). The WE014 is clearly labeled with the chromatographic peaks corresponding to the sample and the impurity of WE017. The sample WE017 is pure.

#### Fourier transformed infrared spectroscopy (FTIR)

Figure 6 shows the comparisons of guanylhydrazones IR spectra at room temperature, intermediate temperatures, and higher temperature. The intermediate temperatures were WE010 (190 °C), WE014 (208 °C), and WE017 (215 °C), before melting temperature. The higher temperature was 300 °C for all samples, before decomposition temperature. These temperatures obtained from the DSC curves were the same.

Based on the analysis of information in Fig. 6, it can be noticed that the first intermediate temperatures for WE010, WE014, and WE017 samples produced spectra comparable with the room temperature spectrum, presenting Pearson correlation values of  $r = 0.83$ ,  $r = 0.75$ , and  $r = 0.70$ , respectively. These results show a high correlation to WE010 ( $r > 0.8$ ), showing no significant differences



**Fig. 5** a DSC curves, b Chromatography peaks of WE010, WE014 and WE017

between the IR spectra of WE010 at room temperature and at the intermediate temperature, thus confirming the thermal results where the melting occurs without decomposition. However, the guanylhydrazones WE014 and WE017 presented Pearson correlation of  $0.5 > r > 0.8$ , which corresponds the moderate correlation between spectrums, that can be attributed to the displacements of some bands, which is in agreement with the decomposition reviewed by the DSC analysis.

The second higher temperature for all samples produced Pearson correlation values of  $r = 0.062$ ,  $0.40$ , and  $0.39$ , respectively. This means that the correlation between room temperature and high temperature spectrum suggesting severe degradation of the original molecular structures. Only WE010 had the mean correlation in the IR fingerprint zone higher than  $0.50$  which indicated probably a less extensive degradation. The thermoanalytic data corroborate the data from the FTIR, confirming the fusion of guanylhydrazones at intermediate temperatures and decomposition at high temperatures.

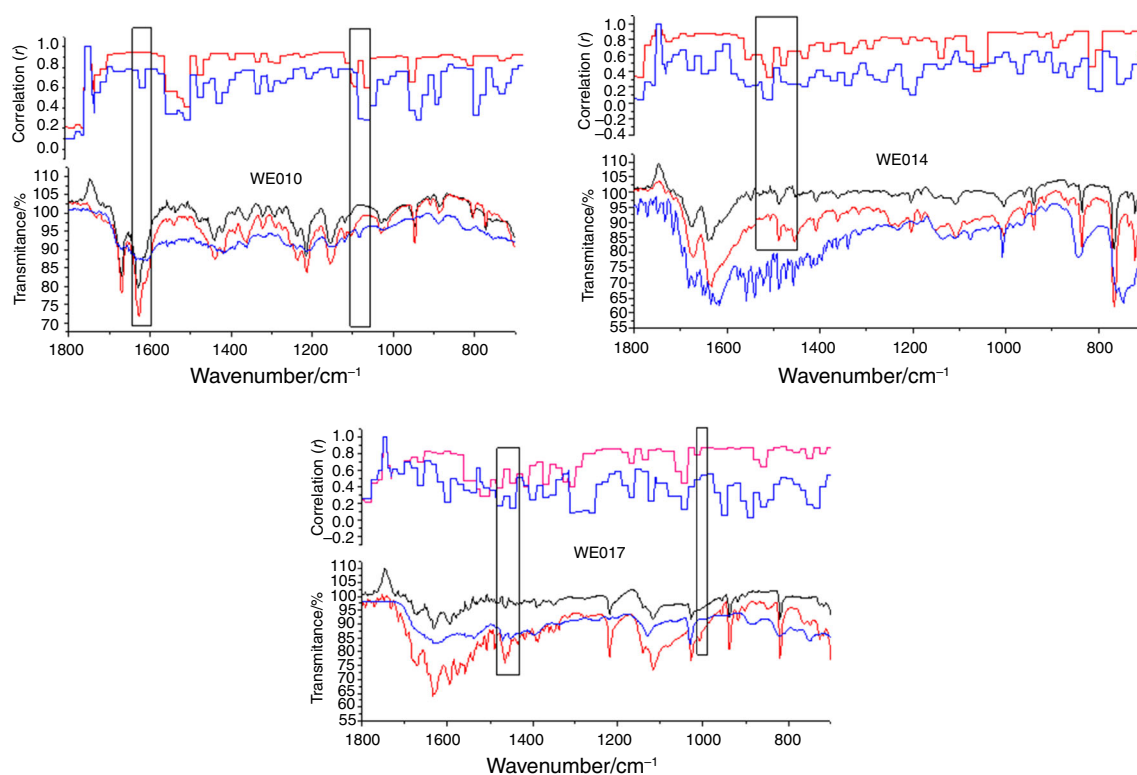


**Fig. 6** Comparisons of IR sample spectra of guanylhydrazones at room temperature (*black line*), intermediate temperatures (*red line*), and higher temperature (*blue line*). The *rectangles* indicate peaks that are considerably different between spectra. (Color figure online)

## Conclusions

The determination of the purity of substances by DSC is considered a fast and reliable process when the melting is not accompanied by thermal decomposition of the compound. Thus, we determined the purity of the WE010 using the melting peak of the sample due to the symmetry found in the sample. In the case of samples WE014 and WE017, characterizations were carried out using the melting peak, but it was not possible to determine the purities of these two samples because the compounds decompose at the subsequent stage of melting. HPLC has confirmed these data. The data from DSC-photovisual confirmed the melting and the presence of impurities in the samples. The use of DSC in the determination of purity of molecules with therapeutic potentials is an efficient and fast method that contributed for quality control of these molecules. The FTIR is a very important technique to confirm the thermal analytical data. Thus, the use of thermal analysis is an important tool for the characterization of molecules with therapeutic potentials, contributing to the characterization and evaluation of their stabilities as well as non-thermal technique with complementary tool.

**Acknowledgements** The authors would like to thank FAPERN/ UFRN for their technical and financial supports for this research.

## References

- Colombo M, Peretto I. Chemistry strategies in early drug discovery: on overview of recent trends. *Drug Discov Today*. 2008;13:15–6.
- Barreiro EJ, Fraga CAM. Química medicinal: as bases moleculares da Ação dos Fármacos. Porto Alegre: ArtMed; 2008.
- Walzer PD, Foy J, Runck J, Steele P, White M, Klein RS, Otter BA, Sundberg RJ. Guanylhydrazones in therapy of *Pneumocystis carinii* pneumonia in immunosuppressed rats. *Antimicrob Agents Chemother*. 1994;38:2572–6.
- Gossnitzer E, Feierl G, Wagner U. Synthesis, structure investigations, and antimicrobial activity of selected *s-trans*-6-aryl-4-isopropyl-2-[2-[(E)-1-phenylalkylidene]-(E)-hydrazino]-1,4-dihydropyrimidine hydrochlorides. *Eur J Pharm Sci*. 2002;15: 49–61.
- Ulrich P, Cerami A. Synthesis, resolution, absolute stereochemistry, and enantioselectivity of 3',4'-dihydroxynomifensine. *J Med Chem*. 1984;27(1):35–40.
- Sundberg RJ, Dahlhausen DJ, Manikumar G, Mavunkel B, Biswas A, Srinivasan V, Musallam HA, Reid WA Jr, Ager AL. Cationic antiprotozoal drugs trypanocidal activity of 2-(4'-formylphenyl)imidazo[1,2-a]pyridinium guanylhydrazones and related derivatives of quaternary heteroaromatic compounds. *J Med Chem*. 1990;33:298–307.
- Papanastasiou I, Tsoinis A, Kolocouris N, Prathalingam SR, Kelly JM. Design, synthesis and trypanocidal activity of new aminoadamantane derivatives. *J Med Chem*. 2004;51:1496–500.
- Andreani A, Granaiola M, Leoni A, Locatelli A, Morigi R, Rambaldi M, Lenaz G, Fato R, Bergamini C, Farruggia G. Potential antitumor agents. *J Med Chem*. 2005;48:3085–9.



9. Foye WO, Alwassian B, Eisenberg MS, Maher TJ. Synthesis and biological activity of guanylhydrazones of 2-pyridine and 4-pyridine and 4-quinoline carboxaldehydes. *J Pharm Sci.* 1990;79(6):527–30.
10. Hoffman BB. Catecolaminas, fármacos simpaticomiméticos e antagonistas dos receptores adrenérgicos. In: Gilman AG, Hardman JG, Limbird LE, editors. *Googman & Gilman: as bases farmacológicas da terapêutica.* 10th ed. Rio de Janeiro: McGraw-Hill; 2003. p. 163–203.
11. Larsen ST, Connell MA, Cudahy MM, Evans BR, May PD, Meglasson MD, Ósullivan TJ, Schostarez HJ, Sih JC, Stevens FC, Tanis SP, Tegley CM, Tucker JA, Vaillancourt VA, Vidmar TJ, Watt W, Yu JH. Synthesis and biological activity of analogues of the antidiabetic/antiobesity agent 3-guanidinopropionic acid: discovery of a novel aminoguanidinoacetic acid antidiabetic agent. *J Med Chem.* 2001;44(8):1217–30.
12. Edmont D. Synthesis and evaluation of quinoline carboxyguanidines as antidiabetic agents. *Bioorg Med Chem Lett.* 2000;10(16):1831–4.
13. Gadad AK, Mahajanshetti CS, Nimbalkar S, Raichurkar A. Synthesis and antibacterial activity of some 5-guanylhydrazone/thiocyanato-6-arylimidazol [2,1-b]-1,3,4-thiadiazole-2-sulfonamide derivatives. *Eur J Med Chem.* 2000;5(9):853–7.
14. Borges MN, Figueroa-Villar JD. NMR interaction studies of aromatic guanylhydrazones with micelles: model for mechanism of action of cationic antibiotics. *Biopolymers.* 2001;62:9–14.
15. Ruiz R, Aviado M. Pharmacology of new antimalarial drugs -3 guanylhydrazones. *Pharmacology.* 1970;4(1):45.
16. Messeder JC, Tinoco LW, Figueroa-Villar JD, Souza EM, Santa Rita R, De Castro SL. Aromatic guanyl hydrazones: synthesis, structural studies and in vitro activity against *Trypanosoma cruzi*. *Bioorg Med Chem Lett.* 1995;5(24):3079–84.
17. Santos Filho AO, Villar JDF, Araújo MT. Molecular modeling of the interaction of trypanocide guanyl hydrazones with B-DNA. *Bioorg Med Chem Lett.* 1997;7(13):1797–802.
18. Epifânio WAN. Síntese e Avaliação Citotóxica de Derivados Aminoguanidínicos Planejados como Protótipos de Fármacos Antineoplásicos. 2011.
19. Medeiros AFD, Santos AFO, de Souza FS, Júnior IDB, Valdiano J, Procópio JVV, de Santana DP, Macêdo RO. Thermal studies of pre-formulates of metronidazole obtained by spray drying technique. *J Therm Anal Calorim.* 2007;89(3):775–81.
20. Gomes APB, Correia LP, Simões MOS, Macêdo RO. Development of thermogravimetric method for quantitative determination of ketoconazole. *J Therm Anal Calorim.* 2008;91(1):317–21.
21. Medeiros AFD, Santos AFO, de Souza FS, Procópio JVV, Pinto MF, Macêdo RO. Thermal stability of paracetamol and its pré-formulates by spray drying. *J Therm Anal Calorim.* 2007;88(2):377–82.
22. Moura EA, Correia LP, Pinto MF, Procópio JVV, de Souza FS, Macêdo RO. Thermal characterization of the solid state and raw material fluconazole by thermal analysis and pyrolysis coupled to GC/MS. *J Therm Anal Calorim.* 2010;100:289–93.
23. Da Silva RMF, de Medeiros FPM, Nascimento TG, Macêdo RO, Neto PJR. Thermal characterization of inidavir sulfate using TG, DSC and DSC-photovisual. *J Therm Anal Calorim.* 2009;95(3):1–4.
24. Procópio JVV, de Souza VG, da Costa RA, Correia LP, de Souza FS, Macêdo RO. Application of thermal analysis and pyrolysis coupled to GC/MS in the qualification of simvastatin pharmaceutical raw material. *J Therm Anal Calorim.* 2011;106:665–70.
25. Pinto MF, Correia LP, de Souza FS, Macêdo RO. Thermal compatibility studies of nitroimidazoles and excipients. *J Therm Anal Calorim.* 2010;102(1):323–9.
26. Gomes APB, Correia LP, Simoes MOS, Macêdo RO. Development of thermogravimetric method for quantitative determination of mebendazole. *J Therm Anal Calorim.* 2007;87(3):919–25.
27. Arora S, Aneja DK, Kumar M, Sharma C, Prakash O. Thermal studies of some biological active oxidazoles. *J Therm Anal Calorim.* 2013;111:17–25.
28. Binil PS, Anoop MR, Suma S, Sudarsanakumar MR. Growth, spectral, and thermal characterization of 2-hydroxy-3-methoxybenzaldehyde semicarbazone. *J Therm Anal Calorim.* 2013;112:913–9.
29. Zianna A, Vecchio S, Gdaniec M, Czapik A, Hatzdimitriou A, Lalia-Kantouri M. Synthesis, thermal analysis, and spectroscopic and structural characterizations of zinc(II) complexes with salicylaldehydes. *J Therm Anal Calorim.* 2013;112:455–64.
30. Carlini R, Macciò D, Pani M, Parodi N, Zanichchi G, Carnasciali MM, Costa GA. Synthesis and thermal properties of NiSbS-As doped phase. *J Therm Anal Calorim.* 2013;112:513–7.
31. Rather MS, Majid K, Wanchoo RK, Singla ML. Synthesis, characterization, and thermal study of polyaniline composite with the photoadduct of potassium hexacyanoferrate(II) involving hexamine ligand. *J Therm Anal Calorim.* 2013;112:893–900.
32. Alghool S, El-Halim HFA, El-Sadek MSA, Yahia IS, Wahab LA. Synthesis, thermal characterization, and antimicrobial activity of lanthanum, cerium, and thorium complexes of amino acid Schiff base ligand. *J Therm Anal Calorim.* 2013;112:671–81.
33. Koshinim M, Elo H, Lukkari P, Riekkola M-L. Determination of the antileukemic drug mitoguazone and seven other closely related bis(amidinohydrazones) in human blood serum by high-performance liquid chromatography. *J Chromatogr B.* 1996;685:141–9.
34. Cerami C, Zhang X, Ulrich P, Blanch M, Tracey KJ, Berger BJ. High-performance liquid chromatographic method for guanylhydrazone compounds. *J Chromatogr B.* 1996;671:71–5.
35. Araújo AAS, Bezerra MS, Storpitis S, Matos JR. Determination of the melting temperature, heat of fusion, and purity analysis of different samples of zidovudine (AZT) using DSC. *Braz J Pharm Sci.* 2010;46:37–43.
36. Fernandes FHA, Santana CP, Santos RL, Correia LP, Conceição MM, Macêdo RO, Medeiros ACD. Thermal characterization of dried extract of medicinal plant by DSC and analytical techniques. *J Therm Anal Calorim.* 2013;113(2):443–7.
37. Pereira MAV, Fonseca GD, Silva-Júnior AA, Fernandes-Pedrosa MF, Moura MFV, Barbosa EG, Gomes APB, Santos KSCR. Compatibility study between chitosan and pharmaceutical excipients used in solid dosage forms. *J Therm Anal Calorim.* 2014;116:1091–100.